Molecular Biology of the Cell
Vol. 16, 4398–4409, September 2005

Inhibition of *Pkhd1* Impairs Tubulomorphogenesis of Cultured IMCD Cells[V]

Weiyi Mai,*† Dong Chen,* Tianbing Ding,* Ingyu Kim,* Sujun Park,* Sae-youll Cho,* Julia S.F. Chu,‡ Dan Liang,* Ning Wang,* Dianqing Wu,§ Song Li,‡ Ping Zhao,‖ Roy Zent,*¶# and Guanqing Wu,*‖@

Departments of *Medicine, @Cell and Developmental Biology, and ¶Cancer Biology, Vanderbilt University, Nashville, TN 37232; §Department of Genetics and Developmental Biology, University of Connecticut, Farmington, CT 06030; ‡Department of Bioengineering, University of California–Berkeley, Berkeley, CA 94720; ‖Laboratory of Translational Cancer Research, Cancer Institute and Hospital, Chinese Academy of Medical Sciences, Beijing 100021, China; #Department of Research Medicine, Veterans Administration Hospital, Nashville, TN 37232; and †Department of Cardiology, First Affiliated Hospital, Sun Yat-sen University, Guangzhou 510080, China

Submitted November 22, 2004; Revised May 16, 2005; Accepted June 15, 2005
Monitoring Editor: Keith Mostov

Fibrocystin/polyductin (FPC), the gene product of *PKHD1*, is responsible for autosomal recessive polycystic kidney disease (ARPKD). This disease is characterized by symmetrically large kidneys with ectasia of collecting ducts. In the kidney, FPC predominantly localizes to the apical domain of tubule cells, where it associates with the basal bodies/primary cilia; however, the functional role of this protein is still unknown. In this study, we established stable IMCD (mouse inner medullary collecting duct) cell lines, in which FPC was silenced by short hairpin RNA inhibition (shRNA). We showed that inhibition of FPC disrupted tubulomorphogenesis of IMCD cells grown in three-dimensional cultures. *Pkhd1*-silenced cells developed abnormalities in cell-cell contact, actin cytoskeleton organization, cell-ECM interactions, cell proliferation, and apoptosis, which may be mediated by dysregulation of extracellular-regulated kinase (ERK) and focal adhesion kinase (FAK) signaling. These alterations in cell function in vitro may explain the characteristics of ARPKD phenotypes in vivo.

INTRODUCTION

Autosomal recessive polycystic kidney disease (ARPKD) is a hereditary nephrohepatic cystic disease that usually occurs in infants and children (Guay-Woodford, 1996; Zerres *et al.*, 1998). The major clinical manifestations of this disease are ectasia of renal collecting and hepatic biliary ducts as well as fibrosis of both the liver and kidneys (Potter, 1972; Bosniak and Ambos, 1975). By genetic linkage analysis, the gene responsible for this disease, termed polycystic kidney and hepatic disease 1 (*PKHD1*), was mapped to human chromosome 6p (Mucher *et al.*, 1994; Guay-Woodford *et al.*, 1995) and was recently cloned by several independent groups (Onuchic *et al.*, 2002; Ward *et al.*, 2002; Xiong *et al.*, 2002). *PKHD1* is speculated to encode a receptor-like protein (Ward *et al.*, 2002) and may be composed of distinct exons that generate a number of isoforms (Onuchic *et al.*, 2002; Xiong *et al.*, 2002). The longest ORF of *PKHD1* (*PKHD1-FP*) contains 67 exons and encodes a 4074-amino acid (AA) membrane-associated protein, termed fibrocystin/polyductin (FPC). In addition, our group identified a short form of *PKHD1*, named *PKHD1-tentative* (*PKHD1-T*), which encodes a 3396-AA protein, termed tigmin (FPT; Xiong *et al.*, 2002).

PKHD1 encodes a very large and complex protein with only a few recognizable motifs and a single predicted transmembrane domain (Onuchic *et al.*, 2002; Ward *et al.*, 2002; Xiong *et al.*, 2002). Using a panel of antibodies, it was shown that PFC is widely expressed in epithelial derivatives, which form the primary duct system during embryogenesis and organogenesis (Nagasawa *et al.*, 2002; Zhang *et al.*, 2004). In the kidney, FPC predominantly localizes to the apical domain of renal tubule cells, where it associates with the basal bodies/primary cilia (Masyuk *et al.*, 2003; Ward *et al.*, 2003; Menezes *et al.*, 2004; Wang *et al.*, 2004; Zhang *et al.*, 2004).

A well known approach in studying the tubulomorphogenic processes is the use of three-dimensional (3-D) epithelial cell cultures in extracellular matrix (ECM) gels (Zegers *et al.*, 2003). To unravel the role of FPC in regulating renal epithelial function, we used stable *Pkhd1*-silenced IMCD cells to characterize its functions in tubulomorphogenesis, cell proliferation, apoptosis, motility, polarization, and cytoskeletal organization. Our results indicate that the expression of normal PFC is required to sustain renal tubulogenesis/tubulomaturation in 3-D cultures of IMCD cells. Lack of this protein resulted in abnormalities in cell-cell contact, actin cytoskeleton organization, cell-ECM interactions, cell proliferation, and apoptosis. *Pkhd1*-silenced IMCD cells showed delayed and diminished ERK1/2 and FAK pY861 activation after cell adhesion to ECM, suggesting that FPC

This article was published online ahead of print in *MBC in Press* (http://www.molbiolcell.org/cgi/doi/10.1091/mbc.E04–11–1019) on June 22, 2005.

[V] The online version of this article contains supplemental material at *MBC Online* (http://www.molbiolcell.org).

Address correspondence to: Guanqing Wu (guanqing.wu@vanderbilt.edu).

may mediate tubulomorphogenesis of IMCD cells via ERK and FAK signaling pathways. The observations made in vitro may illuminate the characteristics of ARPKD phenotypes in vivo.

MATERIALS AND METHODS

MATERIALS

The commercial reagents and antibodies used in this study were as follows. Rat type I collagen (CI) were obtained from Becton Dickinson (Franklin Lakes, NJ). Gelatin (Sigma, St. Louis, MO), pEGFP-Tub MDCK (Clontech, Palo Alto, CA), paraformaldehyde (Sigma), Rhodamine-phalloidin (Vector Laboratories, Burlingame, CA), anti-ZO-1 (Zymed Laboratories, South San Francisco, CA), anti-E-cadherin (BD Transduction Laboratories, Lexington, KY), acetylated α-tubulin (Sigma), p-Akt/total Akt (Cell Signaling Technology, Beverly, MA), p-ERK/total ERK (Cell Signaling Technology), FAKpY397, 407, 576, 577, 861 (BioSource, Camarillo, CA), and total FAK (BD Transduction Laboratories) antibodies were purchased. Polyclonal and monoclonal antibodies against FPC, including hAR-Np, hAR-C2p, hAR-Nm3G12, hAR-Cm3G6, and hAR-C2m3C10, were described in our previous study (Zhang *et al.,* 2004). Secondary antibodies included Cy3-conjugated rabbit anti-mouse IgG, Cy2-conjugated goat anti-rabbit IgG (Jackson ImmunoResearch Laboratories, West Grove, PA), Alexa Fluor 488 goat anti-mouse IgG, and Alexa Fluor 594 goat anti-rabbit IgG (Molecular Probes, Eugene, OR).

METHODS

Cell Culture and Transfection. Culture conditions for IMCD cells and the tubulogenesis assay for the IMCD-derived cells in 3-D ECM gels were as previously described (Zent *et al.,* 2001; Chen *et al.,* 2004). The collagen I (CI) gels were composed of 1 mg/ml CI in Dulbecco's minimal essential medium containing 20 mM HEPES (pH 7.2). The Matrigel/collagen I gels (MG) is 1:1 mixture of CI and MG with a final concentration of 0.5 mg/ml for CI and 0.5 mg/ml for Matrigel (Chen *et al.,* 2004). Ten percent fetal calf serum (FCS) was used for GI and MG gel cultures. The tubule formation was determined in five randomly picked high-power fields (Figure 1, A–D). The cells used to establish normal cell-cell contacts were plated and grown to confluence for at least 3 d on 12-mm transwell plates (Costar, Cambridge, MA). Transient transfection assays were performed in 24- or 6-well culture plates (Costar) with Lipofectamine 2000 (Invitrogen, Carlsbad, CA). The procedures for transfection were performed according to the manufacturer's protocol. All cell culture reagents were purchased from Life Technologies (Invitrogen).

Small Interfering RNA and shRNA Stable Cell Lines. Double-stranded small interfering RNAs (siRNAs) were synthesized by Dharmacon Research (Boulder, CO; Table 1). Subconfluent populations of IMCD cells were transfected using Lipofectamine 2000 according to the manufacturer's instructions. Tubulogenesis assays were performed 24 h after the transfection. To establish stable *Pkhd1*-silenced and control IMCD cell lines, *Pkhd1* siRNA3 and other control constructs (Figure 2A) were transiently transfected into subconfluent IMCD cells. Twenty-four hours later, 5% FCS DMEM/F12 along with G418 at a concentration of 1 mg/ml was used to select for G418-resistant clones. After a week of G418-selective culture, the remaining cells were resuspended and seeded in 100-mm^2 culture plates (Costar) with a cell density of 10^3 per plate. When G418-selected colonies were formed, single colonies were picked using inverted microscopy and transferred into a new set of 24-well cultured plates (Costar).

RNA Isolation and Quantitative PCR. Total RNA was isolated from the IMCD-derived transient transfected cells and stable cell lines using Trizol reagents (Invitrogen) according to the manufacturer's instructions. Quantitative PCR was performed using the iCycler iQ Real Time PCR Detection System (Bio-Rad, Richmond, CA). A pair of primers was designed to bridge exons 34 and 35 in *Pkhd1* cDNA. The forward primer, 5′-GGC TTT CCT ATG TGA CCT G-3′, and reverse primer, 5′-trichloroacetic acid CAC TCC ATC TCT GCC TC-3′ were used for real-time PCR with the iQ SYBR Green Supermix kit (Bio-Rad).

Western Blotting, Immunofluorescence Staining, and Flow Cytometry. The different IMCD cell populations were serum starved for 12 h and detached from the plates with trypsin. The trypsin was inactivated by the addition of 1 mg chicken egg white trypsin inhibitor/ml (Sigma). Cells were then centrifuged and resuspended in serum-free medium. One part of the cells was kept in suspension for 30 min at 37°C, while the other part was replated on collagen I (10 μg/ml) for 10 and 30 min at 37°C, as previously described (Hanks *et al.,* 1992; Cai *et al.,* 2005). Cells were then washed twice with phosphate-buffered saline (PBS) and lysed using RIPA buffer (50 mM Tris-HCl, pH 7.4, 1% Triton X-100, 0.25% sodium deoxycholate, 150 mM NaCl, 1 mM EDTA, protease inhibitor cocktail, 1 mM Na_3VO_4, 1 mM NaF) for 20 min. Lysates were clarified by centrifugation at 12,000 × *g* for 10 min at 4°C. Total protein, 20 μg, was run onto an SDS gel and subsequently transferred to nitrocellulose membranes. Membranes were blocked in 5% milk/tris-buffered saline Tween and then incubated with the different primary antibodies fol-

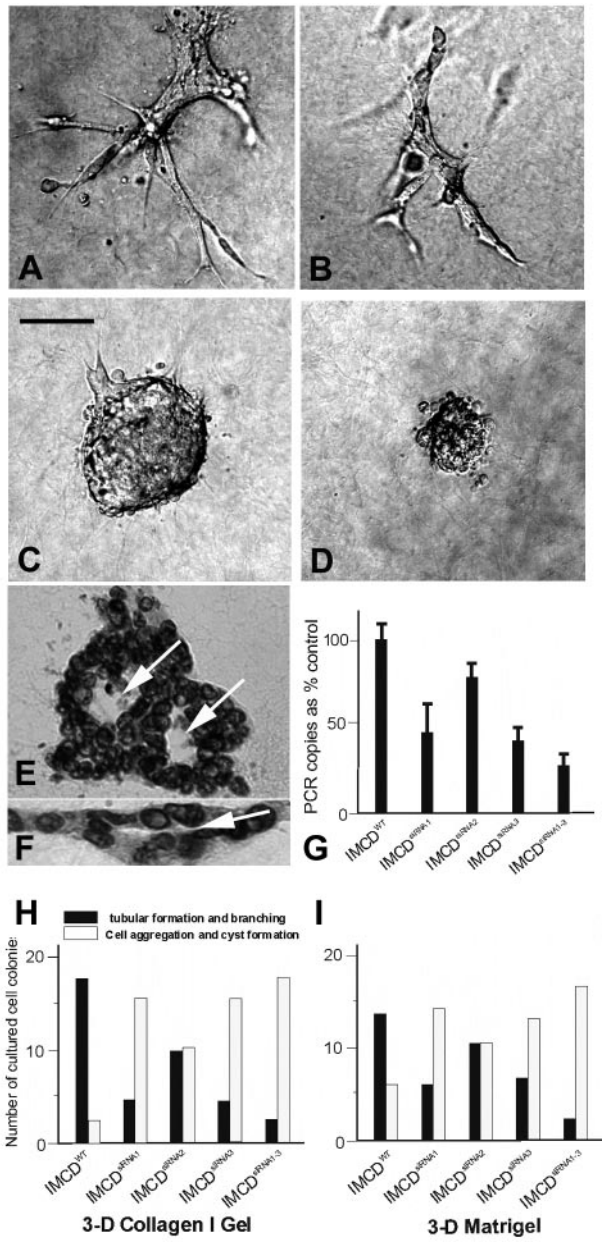

Figure 1. Tubulomorphogenesis of 3-D cultured IMCD cells transiently transfected with dsRNA against FPC. Phase-contrast photomicrographs were taken of examples of wild-type and *Pkhd1*-silenced IMCD cells cultured for 7 d in 3-D CI gels (A–D). Tubulomorphogenesis was seen in IMCD^{WT} cells (A and B) but not *Pkhd1*-silenced IMCD cells (C and D). The tubular lumen was formed under the 3-D culture systems (arrows in E and F). (G) The levels of *Pkhd1* mRNA in IMCD cells transiently transfected with *Pkhd1*siRNAs, including siRNA1, siRNA2, siRNA3 or a mixture of the three called siRNA1–3 (Table 1), were quantified by Real Time PCR Detection System and significant differences were seen between nontransfected and transient transfected cells (* $p < 0.01$). The tubulogenic results from 3-D cultures with CI gels (H) and MG gels (I) are shown. The black bars in H and I refer to tubulogenic structures similar to those seen in A and B and the white bars are cysts or cell aggregates like those seen in C and D. Bar, (A–F) 20 μm.

Table 1. dsRNAs against mouse *Pkhd1*

dsRNA names	dsRNA positions	Sequences
*Pkhd1*siRNA1	Exon 18 (nt1523–34)	5′-AAA CCA CCA TTG AAG AGT AGC-3′
*Pkhd1*siRNA2	Exon 29/30 (nt6442–42)	5′-AAG CAG CAT AGC AGG AGG TGA-3′
*Pkhd1*siRNA3	Exon 34 (nt8564–84)	5′-AAA GTC AGG AGC TCC ACC TAC-3′

lowed by the appropriate HRP-conjugated secondary antibodies. Immunoreactive bands were identified using enhanced chemiluminescence according to the manufacturer's instructions.

For immunofluorescence (IF), cultured cells were first washed with 1× PBS twice and fixed with 4% paraformaldehyde at 4°C for 30 min. The cells were washed twice more with 1× PBS and incubated with 1% bovine serum albumin (BSA) at room temperature for 1 h. The cells were then incubated with primary antibodies for 2 h and washed again with 1× PBS three times. Washed cells were treated with fluorescence-conjugated secondary antibodies for 1 h.

For flow cytometry, a suspension of tested cells was incubated with fluorescent reagents provided in the Apoptosis Kits (BioVision Research Products). Flow cytometry was performed with a FACScan instrument (Becton Dickinson, San Jose, CA).

Confocal Microscopy, Time-lapse Phase-Contrast Microscopy, and Scanning Electron Microscopy. For confocal microscopy, the IF images were collected as *Z*-series sections using a Zeiss LSM 510 confocal microscope system (Thornwood, NY) with a 10× or 40× oil objective. Multiple sections (~0.3–0.5 μm thick) were projected onto one plane for presentation.

Time-lapse microscopy video was performed using a Nikon inverted microscope (TE300; Melville, NY) equipped with a 10× objective. A temperature hood was built around the microscope to keep the temperature at 37°C during experiments. Phase-contrast images were collected using a Hamamatsu

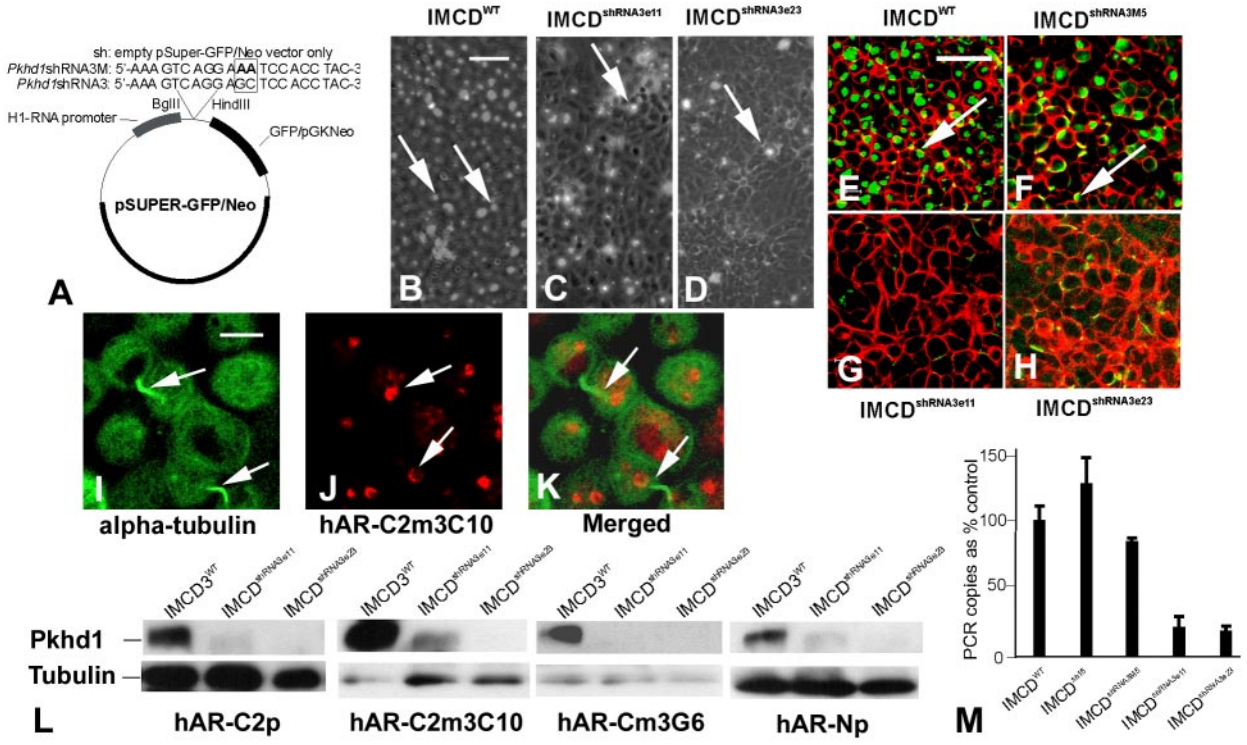

Figure 2. Establishment of stable *Pkhd1*-silenced IMCD cell lines. (A) *Pkhd1*-siRNA3 (Table 1) was inserted into the pSUPER-GFP/Neo vector (sh), which provided the shRNA backbone and was named *Pkhd1*shRNA3. To establish stable control cell lines, two nucleotides in the middle of the duplex were mutagenized from GC to AA, and this was called *Pkhd1*shRNA3M. The pSUPER-GFP/Neo empty vector was also used to produce control cell lines, IMCD^{sh}. (B–D) A monoclonal antibody (mAb) against the N-terminal portion of FPC, hAR-Nm3G12, was used to stain all the tested cell lines. Positive immunoreactivity of the basal bodies/cilia appears as spots (arrows in B–D). The *Pkhd1*-silenced lines, IMCD^{shRNA3e11} (C) and IMCD^{shRNA3e23} (D), showed a significant decrease of FPC in that they had fewer and smaller spots of immunoreactivity than IMCD^{WT} (B). The merged confocal images (E–H) in which IMCD-derived cell lines were costained with rhodamine-phalloidin and a mAb against the C-terminal portion of FPC, hAR-C2m3C10, also showed tremendous reduction of FPC immunoreactivity in the *Pkhd1*-silenced cell lines (G and H), when compared with control cell lines (arrows in E and F). pEGFP-Tub MDCK cells (I), in which EGFP was stably coexpressed with human α-tubulin, were stained with an anti-FPC mAb, hAR-C2m3C10 (J). Confocal merged images showed FPC staining was highly agglomerated at the basal bodies of the cells (arrows in J), whereas primary cilia of the cells (arrows in I) were marked by EGFP-expressed α-tubulin, suggesting that FPC localizes to the vicinity of the basal bodies of cultured renal epithelial cells (arrows in K). (L) The knockdown cell lines (IMCD^{shRNA3e11} and IMCD^{shRNA3e23}) were subjected to Western blotting analysis with a panel of mono- and polyclonal antibodies against FPC. The cell lines showed a significant reduction of FPC protein expression when compared with the wild-type cell line IMCD^{WT}. Protein loading was showed by antitubulin antibody in the same Western blots. (M) Quantitative PCR showed that the levels of *Pkhd1* mRNA in the IMCD^{shRNA3e11} and IMCD^{shRNA3e23} cell lines were significantly lower than in the wild-type and empty-vector IMCD^{sh} control ($p < 0.001$). Notably, the level of mRNA for *Pkhd1* was slightly decreased at ~75% of the wild-type and mutagenized control cell line (IMCD^{shRNA3M5}). Bars, (B–H) 15 μm, (I–K) 5 μm.

Orca100 cooled digital CCD camera (Bridgewater, NJ) at 20-min intervals for 20–24 h and transferred directly from a frame grabber to computer storage using C-Imaging System software (Compix, Cranberry Township, PA). Cell outlines were visualized by phase contrast microscopy with a 10× objective. A scanning stage allowed image collection from different areas of the sample automatically.

For scanning electron microscopy, samples were fixed in 2% glutaraldehyde in 0.1 M sodium cacodylate for 1 h followed by treatment with 1% osmium tetroxide in 0.1 M sodium cacodylate buffer. After an ethanol dehydration series, the samples were critical-point dried and sputter-coated with 40% gold, 60% palladium microparticles to a thickness of 15–17 nm. The images of the samples were collected by using an Electroscan E3 Environmental Scanning Electron Microscope (Hitachi S-5000, Hitachi Science, Ibaraki, Japan).

Cell proliferation and Apoptosis. IMCD cells (3×10^3) were embedded in the 3-D gels (100 μl final volume) in 96-well plates as described above and incubated in DMEM/F12 containing 5% FCS. After 2 d in culture, cells were pulsed for an additional 48 h with [^{3}H]thymidine (1 μCi/well). The gels were then removed from the plates and dialyzed against PBS for 24 h to remove free [^{3}H]thymidine. The cells in the gels were then lysed in 1% SDS (100 μl final volume) and the lysates were measured with a β counter. In addition, the Quick Cell Proliferation Assay Kit (BioVision Research Products) was used to analyze the proliferation rate among the cell lines. This assay is based on cleavage of the tetrazolium salt WST-1 to formazan by cellular mitochondrial dehydrogenases. Expansion of the number of viable cells results in an increase in the activity of the mitochondrial dehydrogenases (Berridge *et al.*, 1996), leading to an increase in the amount of formazan dye, which can be detected by spectrometry.

For apoptosis studies, the cells were incubated in 3-D gels as described above. After 7 d in culture, the gels were fixed in 4% paraformaldehyde for 30 min, followed by dimethyl sulfoxide/methanol at a ratio of 1:1 for 30 min. Apoptosis was detected using the Apoptag Apoptosis Detection Kit as described by the manufacturer (Serologicals, Norcross, GA). The gels were also stained with DAPI to identify all the cell nuclei. Apoptotic cells were counted in at least 10 different microscopic fields of a fluorescence microscope and the apoptotic index, expressed as (number of positive apoptotic cells/200 counted cells) × 100, was determined. We also quantified apoptosis using an Annexin V-PE Apoptosis Kit (BioVision Research Products), in which Annexin V is conjugated to PE as the florescent marker (An and Huang, 2004) to evaluate apoptotic rates by flow cytometry.

Cell Adhesion and Migration Assays. The 96-well cell culture plates (Nunc, Napierville, IL) were coated with CI at the indicated concentrations in PBS for 12 h at 4°C. The negative controls were performed on plates coated with 1% BSA. Positive controls were the cells plated onto tissue culture plates in the presence of 10% FCS. The plates were then washed with PBS and incubated with PBS containing 1% heat-denatured BSA for 60 min to block nonspecific adhesion. Aliquots (100 μl) of single-cell suspensions (10^6 cells/ml) in serum-free DMEM/F12 containing 0.1% BSA were added in triplicate to 96-well plates with 0.01–2 μg/ml CI and incubated for 60 min at 37°C. Nonadherent cells were removed by washing the wells with PBS. Cells were then fixed with 4% formaldehyde, stained with 1% crystal violet, solubilized in 20% acetic acid, and the OD of the cell lysates was read at 570 nm. Cells bound to FCS were used as a positive control to indicate maximal cell adhesion, and the amount of cells bound to CI-uncoated wells (BSA only) was used as the background, and this OD was subtracted from that obtained with serum or ECM proteins. We evaluated the cell-matrix adhesion by the formula: (OD value of tested cells minus OD of background/OD of positive controls minus OD of background) × 100.

Transwell filter migration assay was performed in polyvinylpyrolidone-free polycarbonate filters with 8-μm pores (Costar). The underside of the transwell was precoated with 5 μg/ml CI overnight at 4°C and the filter was subsequently blocked with 1% BSA for an hour at 37°C to inhibit nonspecific migration. Aliquots (100 μl) of cell suspension (1×10^6 cells/ml) in serum-free medium were added to the wells, and cells were allowed to migrate into the matrix coated on the underside of the transwell for 3 h. Cells on the top of the filter were removed by wiping and the filter was then fixed in 4% formaldehyde in PBS. Migrating cells were stained with 1% crystal violet and five randomly chosen fields from triplicate wells were counted at 200× magnification.

A wound-healing assay was used to test the cell migration in the IMCD cell lines and the cells (10^4 cells/well) were seeded in 24-well culture plates with low serum (0.5%). After 2 d of culture, the confluent monolayers were wounded by scraping a 10–15-μm line with a flattened needle across the cell monolayer. The status of the wound line was then documented by time-lapse microscopy at 20-min intervals for >12 h.

Histological Sectioning of Cultured Gels. The 3-D cultured samples were washed with 1× PBS twice, then fixed with 4% paraformaldehyde, and incubated at room temperature for 20 min. After a regular ethanol dehydration series, the samples were treated twice with xylene for 20 min each time and then soaked in 1:1 xylene/paraffin for 30 min followed by paraffin alone for 30 min. The paraffin-embedded samples were then sectioned to a thickness of 6 μm using a Leica 2135 microtome (Deerfield, IL).

Transepithelial Resistance. The tested cells were plated on transwell filters (12 well, 0.4-μm pore size, Corning Costar) with 1×10^5 cells per well and allowed to attach overnight, to form a confluent monolayer in normal culture medium. Transepithelial resistance (TER) was measured after 24 h of plating and every 24 h thereafter using an EVOM/STX2 (World Precision Instruments, Sarasota, FL) electrical resistance measurement system with the results expressed in Ω/cm^2.

Statistics. All assays were repeated at least three times in duplicate or triplicate and the graphic data were presented as the mean ± SD. Statistical analysis was performed where appropriate using the Student's *t* test or one-way analysis of variance (ANOVA) followed by the Tukey's Multiple Comparison Test. Differences with $p < 0.05$ were considered statistically significant.

RESULTS

dsRNA-mediated Inhibition of Pkhd1 Impairs Tubule Formation

IMCD cells are polarized mouse renal tubular epithelial cells that undergo tubulogenesis with formation of a lumen (Figure 1, E and F) in 3-D CI and MG gels (Figure 1, A and B; Chen *et al.*, 2004). To test whether silencing FPC would induce abnormal tubulomorphogenesis in 3-D IMCD cell cultures, we selected at least three siRNA duplexes based on the mouse *Pkhd1* cDNA sequence using Oligoengine (Table 1; Zhang *et al.*, 2004). The cDNA fragments for these siRNA duplexes were first used as the query sequence in a BLAST search on the NCBI database to confirm the absence of homology for either humans or mice. Each duplex was then transiently transfected into IMCD cells and 24 h later the cells were placed into 3-D ECM gels for the tubulogenesis assay. The cells transfected with any of the individual siRNA duplexes (Table 1) exhibited decreased *Pkhd1*-mRNA levels with *Pkhd1*siRNA3 resulting in the most *Pkhd1* inhibition (Figure 1G). A combination of all three siRNA duplexes (siRNA1–3) showed the largest amount of inhibition when compared with individual transfections. Tubulogenesis failure (Figure 1, C and D) was present in ~10% in wild-type IMCD cells; however, it was ~85% in *Pkhd1*siRNA1 cultures, 50% in *Pkhd1*siRNA2 cultures, 85% in *Pkhd1*siRNA3 cultures, and 90% in combined *Pkhd1*siRNA1–3 cultures (Figure 1H). Similar results were seen when the cells were seeded in MG gels (Figure 1I). These findings support the idea that silencing *Pkhd1* arrests tubulogenesis in 3-D cultured IMCD cells.

Establishment and Characterization of Stable Pkhd1-silenced IMCD Cell Lines

As inhibition of *Pkhd1* mRNA in the IMCD cells transiently transfected with the *Pkhd1*siRNA3 duplex were profound (Figure 1G), this duplex was selected for constructing a *Pkhd1*shRNA vector, designated the *Pkhd1*shRNA3 clone (Figure 2A). In parallel, we constructed a control vector, *Pkhd1*shRNA3M, in which two nucleotides in the middle of the duplex were randomly mutagenized from GC to AA (Figure 2A). We transfected the *Pkhd1*shRNA3, *Pkhd1*shRNA3M constructs as well as an empty shRNA vector into IMCD cells to produce stable cell lines designated as IMCD^{shRNA3}, IMCD^{shRNA3M}, and IMCD^{sh} (Figure 2A).

We then isolated 12 single G418-resistant clones and performed Western blot analysis and IF staining to select clones of IMCD^{Pkhd1shRNA3} transfected cells in which the expression level of FPC was reduced. Of the 12 selected IMCD^{Pkhd1shRNA3} cell clones, where the *Pkhd1*shRNA3 construct was confirmed by PCR, at least four demonstrated significantly decreased expression of *Pkhd1* mRNA. Two of them, e11 (IMCD^{shRNA3e11}) and e23 (IMCD^{shRNA3e23}), were chosen for further analysis and were eventually used for the functional studies of FPC. Using a similar approach, two

control cell lines were established from the IMCD^{shRNA3M} transfected cells, named IMCD^{shRNA3M5} and IMCD^{shRNA3M9}, and another two empty-vector control cell lines were also established and named IMCD^{sh15} and IMCD^{sh21} (Figure 2A).

Using antibodies against FPC (Zhang *et al.*, 2004), IF cell staining showed that the two *Pkhd1*-silenced IMCD cell lines, IMCD^{shRNA3e11} and IMCD^{shRNA3e23}, exhibited markedly less staining of the basal bodies/cilium than the IMCD wild-type cells (IMCD^{WT}; Figure 2, B–H). The staining patterns in the vector control cell lines (IMCD^{sh15} and IMCD^{sh21}) were similar to the pattern in IMCD^{WT} (Figure 2, B and E). Western blot analysis using both mono- and polyclonal antibodies showed that these two stable *Pkhd1*-silenced cell lines exhibited greatly decreased levels of FPC (Figure 2L). These results provide evidence that FPC was down-regulated in the stable cell lines mediated by the shRNA approach.

Consistent with results from Western analyses, a 4–5-fold decrease in the *Pkhd1* mRNA level was also seen in the IMCD^{shRNA3e11} and IMCD^{shRNA3e23} cells by quantitative PCR, but not in the control cell lines ($p > 0.05$; Figure 2M). In contrast, there was only a 25% decrease in *Pkhd1* mRNA levels (Figure 2M) and relatively less *Pkhd1*-staining (Figure 2F) in IMCD^{shRNA3M5} cells. This result implies that the mutagenized *Pkhd1*-shRNA construct may produce micro-RNA (miRNA) against *Pkhd1* because of its nine identical nucleotides for *Pkhd1* in the construct (Figure 2A). Given that the empty shRNA-vector cell lines did not demonstrate any inhibition effects, whereas mutagenized *Pkhd1*-shRNA and true *Pkhd1*-silenced constructs (*Pkhd1*shRNA3) resulted in minor and strong inhibition, respectively, we can conclude *Pkhd1*shRNA3 silencing activity is specific.

FPC Is Required for Normal Tubulogenesis in 3-D Culture of IMCD Cells

To confirm the finding from the *Pkhd1*siRNA transient transfection assays (Figure 1, H and I), the stably *Pkhd1*-silenced IMCD cell lines were used for tubulogenesis assays. Loss of tubulogenesis was consistently seen in the cultures of *Pkhd1*-silenced cells. Cells failed to establish tubulogenesis in 2–4% of the IMCD^{WT}, 85–95% of the IMCD^{shRNA3e11}, 75–85% of the IMCD^{shRNA3e23}, and <10% of the IMCD^{shRNA3M5} and IMCD^{shRNA3M9} of the CI (Figure 3A) and MG (Figure 3B) 3-D cultures. The significant inhibition of tubulogenesis observed in the *Pkhd1*-silenced cell lines, together with the results from our transient *Pkhd1*-dsRNA-mediated assays, strongly suggest that reduction of FPC expression prevents tubule formation and arrests normal branching morphogenesis in 3-D cultures.

Lack of Pkhd1 Impairs Cell-Cell Contacts

The establishment of intercellular junctions and normal cytoskeletal assembly is essential for epithelial polarity and tubule formation (Higashiyama *et al.*, 1995; Matter and Balda, 2003; Zegers *et al.*, 2003). We therefore assessed the effects of *Pkhd1*-silencing on these cell biological processes.

The subcellular localization and distribution of E-cadherin and ZO-1 were compared between wild-type/control and *Pkhd1*-silenced IMCD cells utilizing immunofluorescence staining. In the wild-type and empty-vector control cell lines, E-cadherin was predominantly seen at the cell-cell junctions (Figure 4A, a and b), whereas in the *Pkhd1*-silenced cells, the junctional staining was markedly indistinguishable and more cytosolic in their subcellular distribution (Figure 4A, d and e). In the mutagenized IMCD^{shRNA3M} clones, the E-cadherin was also predominantly concentrated at the cell-

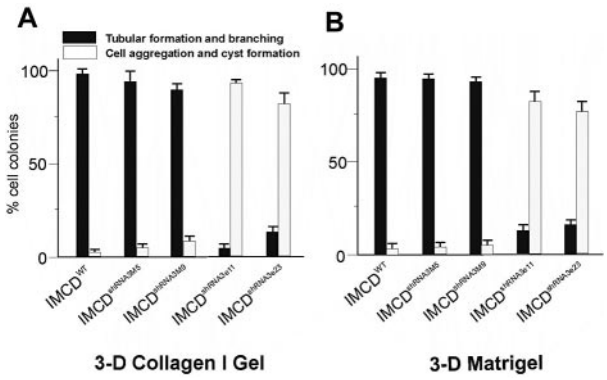

Figure 3. Tubulomorphogenesis is inhibited in *Pkhd1*-silenced IMCD cell lines in 3-D cultures. All the tested cell lines were grown in 3-D CI (A) and MG (B) gels as described in Figure 1. A significantly higher rate of cyst formation and cell aggregation was seen in the IMCD^{shRNA3e11} and IMCD^{shRNA3e23} cells when compared with either wild-type cells or the mutagenized controls IMCD^{shRNA3M5}, IMCD^{shRNA3M9} ($p < 0.001$). The bars and error lines represent the mean and SE of three experiments performed in triplicate.

cell junctions, but some of the cell-cell junctions exhibited a slightly diffused staining pattern (Figure 4Ac). These data from the serial cell lines provide evidence that silencing *Pkhd1* alters the distribution of E-cadherin and impairs the formation of adherent junctions.

To determine whether there were also abnormalities at the tight junctions, the cells were stained with an antibody against ZO-1 (Matter and Balda, 2003). ZO-1 was predominantly found at cell-cell junctions in wild-type cells (Figure 4Ba). In the *Pkhd1*-silenced IMCD cells, junctional staining of ZO-1 showed a diffuse submembranous distribution pattern (Figure 4Bd). As with E-cadherin, ZO-1 staining in the mutagenized IMCD^{shRNA3M} clones was different from the wild-type and empty-vector control cell lines (Figure 4Bc). These results indicate that lack of FPC may also affect the structure of tight junctions.

Given the fact that IF staining showed different distribution patterns for E-cadherin and ZO-1 in wild-type/control versus *Pkhd1*-silenced IMCD cells, we performed a Western blot analysis to determine whether there was a variation in the E-cadherin or ZO-1 expression levels among the different cell lines. There was no detectable immunoreactive change of both proteins between cells with and without down-regulation of FPC (unpublished data), suggesting that FPC alters the cellular distribution of these proteins rather than their levels of expression.

To characterize the functional consequences of these alterations in cell-cell interactions, we measured cell TER. In contrast to the wild-type and control cell lines, TER was low in *Pkhd1*-silenced cells after 3 d of transwell culture ($p < 0.01$) and this persisted out to day 6 (Figure 4C). These results suggest that *Pkhd1*-silenced cells lose the ability to establish normal cell-cell contacts.

Because the cell-cell interactions in the cultured *Pkhd1*-silenced IMCD cells appeared to be abnormal, we hypothesized that down-regulation of FPC might alter the cytoskeleton of these cells. We therefore performed rhodamine-phalloidin staining on the cells. As predicted, we found that the inhibition of FPC disturbed the normal cortical distribution of actin cytoskeleton, resulting in lamellipodia formation (Figure 4D, a and b vs. c). These findings indicate that lack of FPC is able to alter the cytoskeletal organization and induce epithelial to mesenchymal transformation (EMT).

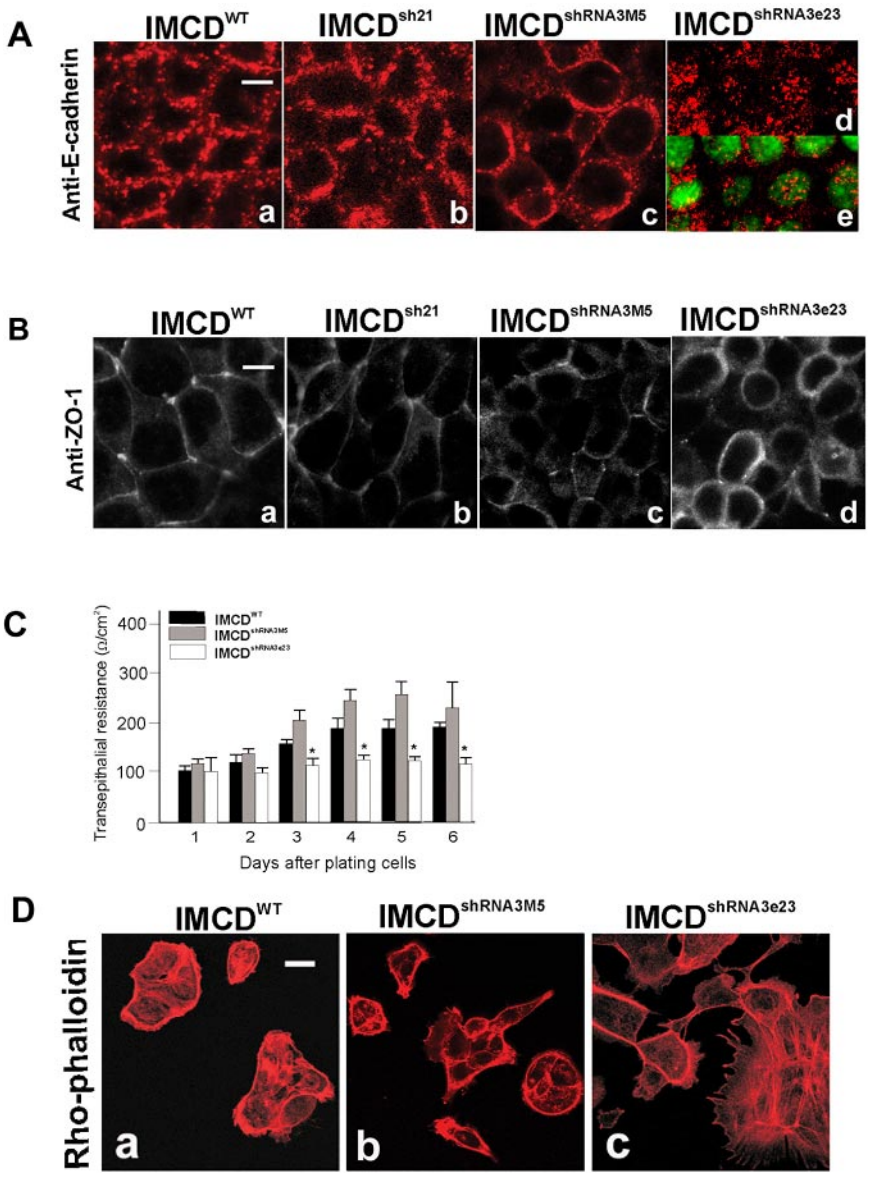

Figure 4. Reduction of FPC alters cell-cell adhesion and disorganizes the actin cytoskeleton. (A) Wild-type ($IMCD^{WT}$), empty vector control ($IMCD^{sh21}$), mutagenized control ($IMCD^{shRNA3M5}$), and knockdown ($IMCD^{shRNA3e23}$) IMCD cells were stained with an antibody to E-cadherin. Confocal images stained with anti-E-cadherin antibody indicated a diffused E-cadherin distribution in cultured *Pkhd1*-silenced cells (A, d–e). Costaining with a dye for nucleic acids, YO-PRO was used in Ae. (B) Tight junction integrity was assessed in the same set of cells tested in A using an anti-ZO-1 antibody. (C) Transepithalial resistance (TER) of the same panel of the cell lines was measured on transwells over a 6-d period. Values showed represent the mean and SD of at least three independent experiments. Significant differences of TER in *Pkhd1*-silenced IMCD cells were observed after 3 d of culture. (* $p < 0.05$). (D) The actin cytoskeleton in $IMCD^{WT}$, $IMCD^{shRNA3M5}$, and $IMCD^{shRNA3e23}$ cell lines was stained using rhodamine-phalloidin. Bars, (A, B, and D) 5 μm.

Down-regulation of Pkhd1 Induces Aberrant Cell Motility

Based on the morphological changes seen in the *Pkhd1*-silenced IMCD cells with respect to cell-cell interactions and the actin cytoskeleton, we examined the motility of the cells in a scratch wound assay on tissue culture plastic in the presence of 0.5% serum. Wound healing in the *Pkhd1*-silenced IMCD cells ($IMCD^{shRNA3e11}$ and $IMCD^{shRNA3e23}$) was only slightly faster than control cells ($IMCD^{sh}$ and $IMCD^{shRNAM5}$) and only the $IMCD^{shRNA3e11}$ clone was statistically significant ($p < 0.05$; Figure 5B). It was noted that *Pkhd1*-silenced cells in margins of the wound were markedly lamellipodial in appearance and did not grow in tight apposition to each other as seen in wild-type IMCD cell cultures (Figure 5A, e and f vs. g and h). To further determine the cell motility of these cell lines, time-lapse microscopy was performed to trace the movement of single cells on tissue culture plastic for 3 h. In this assay *Pkhd1*-silenced IMCD cells showed a faster migration rate than that of control cell lines (Figure 5C).

To demonstrate if the inhibition of FPC induced aberrant migratory polarity in the *Pkhd1*-silenced cells, time-lapse microscopy was performed on cell colonies that were grown on 0.2% gelatin-coated culture plates and photographed at 20-min intervals for >20 h. Intriguingly, the *Pkhd1*-silenced IMCD cells exhibited spontaneous scattering of the cell colonies (Figure 5D, a–c, Supplementary Video S1), developed a fibroblast-like appearance, and migrated away from each other. In contrast, the wild-type and mutagenized control cells exhibited clustered-cell growth and collective cell migration (Figure 5D, d–i and Supplementary Videos S2 and S3). Taken together, these data suggest that the *Pkhd1*-silenced IMCD cells become less epithelial-like than IMCD controls and have undergone a mesenchymal transformation.

Inhibition of the Pkhd1 Gene Product Decreases Integrin-dependent Cell Adhesion

It is well known that cell-ECM interactions play a critical role in branching morphogenesis and perturbations of these interactions in IMCD cells result in decreased branching morphogenesis (Balda and Matter, 2003; Chen *et al.*, 2004). For this reason we investigated the effects of silencing *Pkhd1* in IMCD cells on integrin-dependent adhesion to CI. Cells in

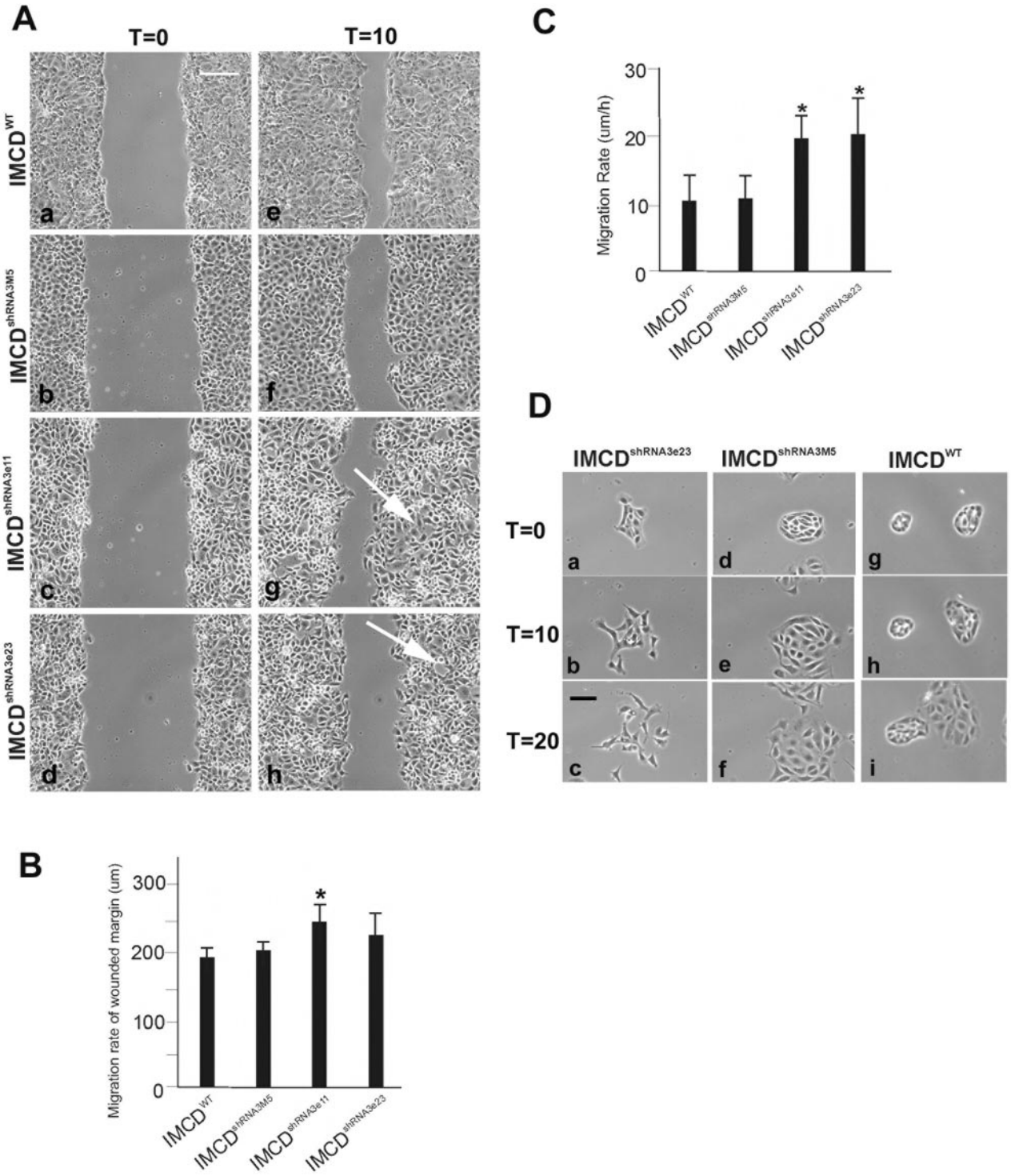

Figure 5. Reduction of FPC induces cell scattering. (A) Wild-type ($IMCD^{WT}$), mutagenized control ($IMCD^{shRNA3M5}$), and knockdown ($IMCD^{shRNA3e11}$ and $IMCD^{shRNA3e23}$) cell lines were grown in 0.5% FCS to confluence on plastic plates and a wound was produced by scratching. Time-lapse images of the wound gaps were taken at initiation of the wounding (a–d) and 10 h after wounding (e–h). The knockdown cell lines (g and h) showed slightly more healing than the wild-type (e) and mutagenized control cell lines (f); however, only $IMCD^{shRNA3e11}$ cell lines had a statistical difference from the wild-type and mutagenized control cell lines (* $p < 0.05$ in B). Notably, the submarginal cells in the *Pkhd1*-silenced IMCD cell lines markedly exhibited loose cell contacts (arrows in g and h) and a lamellipodial appearance compared with the control cell lines (e and f). (C) IMCD cells with or without *Pkhd1*-silencing were placed onto gelatin-coated plates and subjected to time-lapse recording for 3 h. At least five single individual cell for the tested cell lines were traced and their migration rates were shown (E; * $p < 0.01$). (D) Video recordings were also performed on the same panel of cell lines. The studies were initiated 1 h after seeding the cells (a, d, and g). Further photographs at 10 h (b, e, and h) and 20 h (c, f, and i) were taken. Wild-type ($IMCD^{WT}$) and mutagenized control ($IMCD^{shRNA3M5}$) cell lines exhibited collective cell migration (d–i), whereas the *Pkhd1*-silenced IMCD cell lines clearly displayed spontaneous cell scattering (a–c). Bars, (A) 20 μm, (D) 15 μm. A movie of these cell behaviors are presented in Supplementary Videos S1–S3.

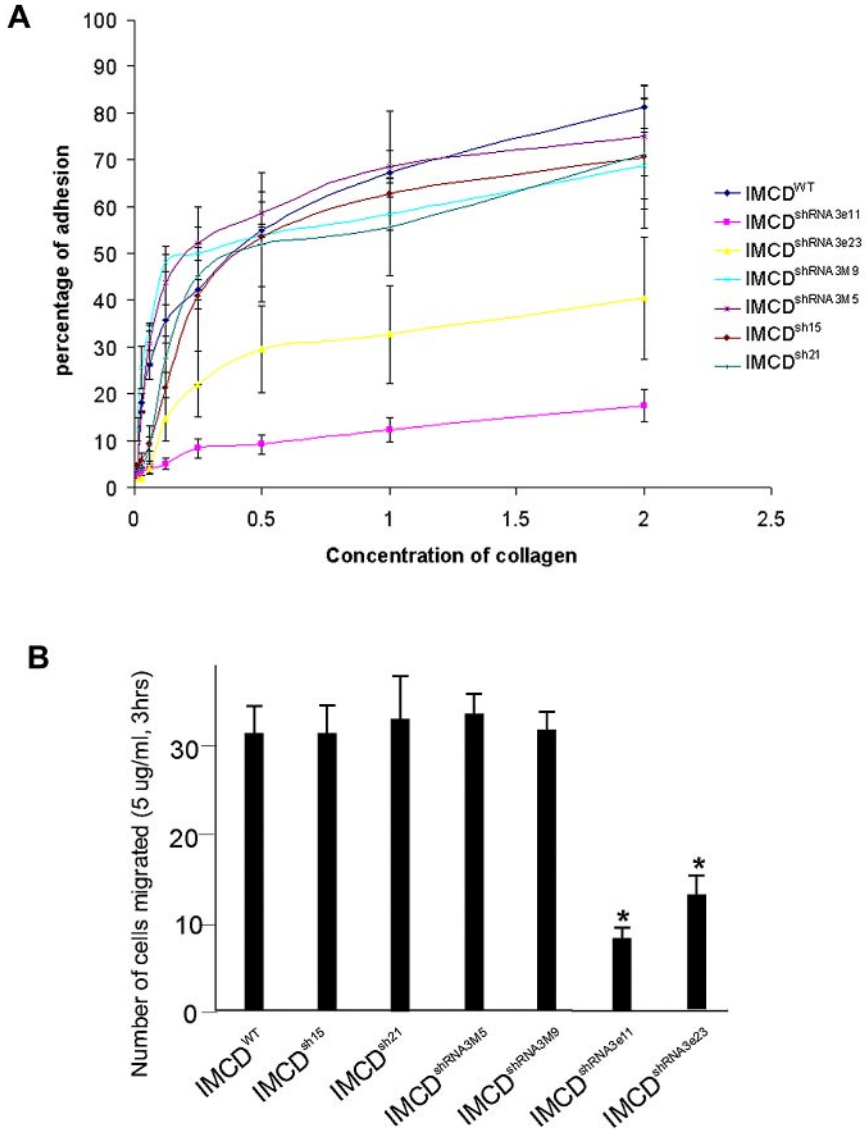

Figure 6. Reduction of FPC decreases integrin-dependent adhesion on CI. (A) Adhesion assays were performed on CI-coated plates as described in *Materials and Methods.* The values shown represent the mean and SD of at least three independent experiments. Significant differences of CI-dependent cell adhesion were seen between the *Pkhd1*-silenced cells and wild-type/controls. (B) CI-induced migration assays were performed on transwell filters as described in *Materials and Methods.* The absolute number of cells that migrated to the underside of the transwell is shown on the *y*-axis. There were significant differences in CI-induced cell migration between cells with and without *Pkhd1*-silencing (* $p < 0.001$).

which *Pkhd1* is silenced adhere less well than control cells at concentrations of CI from 0.1 to 2 μg/ml (Figure 6A). At 2 μg/ml, the IMCD^{shRNA3e11} and IMCD^{shRNA3e23} cells showed only 20–40% cell adhesion compared with >70% for all control cell lines ($p < 0.001$). To identify the importance of FPC on integrin-dependent cell migration, we performed transwell migration assays on CI. As shown in Figure 6B, the *Pkhd1*-silenced cells migrated significantly less than the control groups ($p < 0.05$). These results indicated that inhibition of FPC disrupts integrin-mediated cell interactions.

Reduction of FPC Inhibits Cell Proliferation and Induces Apoptosis in Cultured IMCD Cells

During the time-lapse microscopy examination we observed that the *Pkhd1*-silenced cells proliferated significantly less than the control cells (Supplementary Videos S1–S3). To further validate this finding, we performed proliferation assays in the 3-D CI gels. Knocking down *Pkhd1* resulted in a significant decrease in tritiated thymidine uptake ($p < 0.01$), indicating that the elimination of FPC inhibits cell proliferation (Figure 7A). Similar results were obtained with another proliferation assay, in which the activity of cellular mitochondrial dehydrogenases is measured based on cleavage of the tetrazolium salt WST-1 to formazan (Berridge *et al.*, 1996; Figure 7B). Taken together these assays indicate that lack of FPC suppresses cell proliferation.

Knowing that programmed cell death is associated with tubulomorphogenesis (Zegers *et al.*, 2003) and polycystic kidney disease (Woo, 1995, Boletta, 2000), apoptosis of cells with and without *Pkhd1*-silencing were assessed and quantified by TUNEL assays in the 3-D CI gels. Only 5–10% of the wild-type and control cells underwent programmed cell death, whereas >25% of the *Pkhd1*-silenced IMCD cells underwent apoptosis ($p < 0.001$; Figure 7C). To further confirm the results from the TUNEL assay, we used Annexin V as an indictor to detect programmed cell death in all the tested cell lines (Figure 7D). In agreement with the results from the TUNEL assay, the apoptosis rate seen in the *Pkhd1*-silenced IMCD cell lines was significantly higher than wild-type and all the control cells ($p < 0.001$). These results suggest that inhibition of FPC, either directly or indirectly, promotes

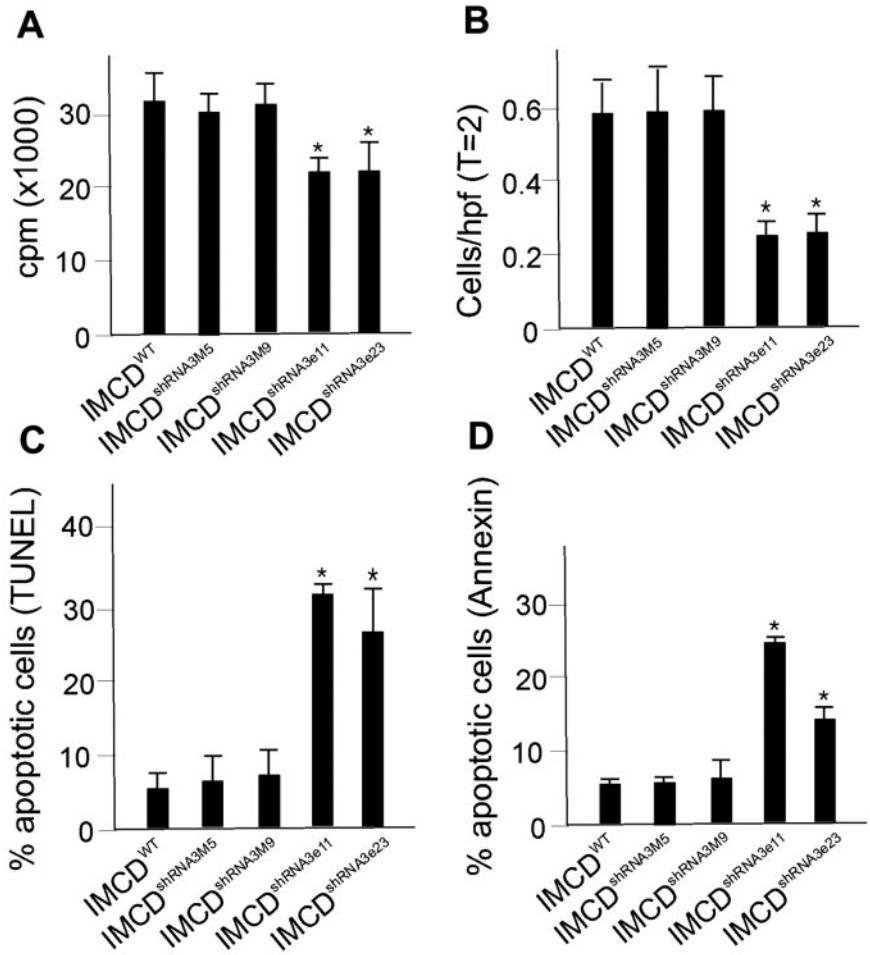

Figure 7. Down-regulation of FPC alters the proliferation and apoptosis of IMCD cells. (A) Wild-type ($IMCD^{WT}$), mutagenized ($IMCD^{shRNA3M5}$ and $IMCD^{shRNA3M9}$), and knockdown ($IMCD^{shRNA3e11}$ and $IMCD^{shRNA3e23}$) IMCD cells were grown in 3-D CI gel for 2 d and then incubated with [^{3}H]thymidine, after which the rate of [^{3}H]thymidine incorporation was determined as described in *Materials and Methods*. [^{3}H]thymidine values were significantly different between cells with and without *Pkhd1*-silencing (* $p < 0.01$). (B) The same tested cells were grown in 96-well plates with the same number of cells per well. Cell proliferation was evaluated according to the procedure in the manual for the Quick Cell Proliferation Assay Kit. Differences in cell proliferation rates were obtained between cells with and without *Pkhd1*-silencing (* $p < 0.01$). (C) All the tested cells were grown in 3-D CI gels; they were then fixed and subjected to TUNEL assays to assess apoptosis as described in *Materials and Methods*. The values represent the percentage of apoptotic cells relative to the total number of cells in the gels. Differences between cells with and without *Pkhd1*-silencing were significant (* $p < 0.001$). (D) All tested IMCD cells were grown in 60-mm plates with the same number of cells per plate for 24 h. An Annexin V-PE staining kit (BioVision) was used to measure the apoptosis rate, according to the manufacturer's instructions. After incubation for 5 min at 37°C, the fluorescence intensity was determined using flow cytometry. An increase in the fluorescence intensity was seen in the *Pkhd1*-silenced cells (* $p < 0.001$). Bars and error lines are the mean and SE of three experiments performed in triplicate.

programmed cell death during tubulomorphogenesis in vitro.

Stable Pkhd1-silenced IMCD Cells Exhibit Aberrant Ciliogenesis

FPC has recently been demonstrated to localize to the primary cilium and/or basal bodies of renal tubular epithelia (Masyuk *et al.*, 2003; Ward *et al.*, 2003; Menezes *et al.*, 2004; Wang *et al.*, 2004; Zhang *et al.*, 2004) and malformation of this cell organelle has been shown to induce cyst formation in the kidneys (Yoder *et al.*, 2002; Lin *et al.*, 2003). We therefore determined whether a lack of FPC arrests ciliogenesis in cultured renal epithelial cells. To this end, scanning electron microscopy (SEM) was used to examine the primary cilia in cells with or without *Pkhd1*-silencing. In contrast to wild-type/control cells (Figure 8A), ciliary formation is markedly suppressed in *Pkhd1*-silenced cells (Figure 8B). Additionally, when a common ciliary marker, acetylated anti-α-tubulin antibody, was used to determine the existence of ciliary malformation in cultured *Pkhd1*-silenced cells, 92% of wild-type IMCD cells showed ciliary staining, whereas *Pkhd1*-silenced IMCD cells displayed <10% staining (Figure 8, C and D). Compared with control cell lines $IMCD^{shRNA3M5}$ and $IMCD^{sh21}$ (Figure 8, E and F), *Pkhd1*-silenced IMCD cells also showed shorten ciliary structure and decreased ciliary staining (Figure 8G). The fact that severe ciliary shortness and absence were found in *Pkhd1*-silenced IMCD cells but not in wild-type/control cells (Figure 8H) suggests that lack of FPC may cause defects in ciliogenesis of renal epithelial cells in vitro.

Abnormal Cellular Phenotypes in Pkhd1-silenced IMCD Cells May Be Mediated by Aberrant ERK and FAK Signaling Pathways

In vitro experiments have shown that tubulomorphogenesis in renal epithelial cell cultures is regulated by the initiation of morphogenetic growth factors that direct cell migration, proliferation, and apoptosis, and in turn modulate cellular reorganization (Nelson, 2003). To determine which putative signaling regulators are most likely to be involved in the processes of FPC-induced tubulomorphogenesis, we examined FAK, JNK/SAPK, PKB/Akt, and ERK1/2 phosphorylation activities, which could be responsible for aberrant cell migration, proliferation, and apoptosis in *Pkhd1*-silenced IMCD cells. Significant differences between wild-type/control and *Pkhd1*-silenced IMCD cells were only seen in ERK and FAK activation. ERK was strongly phosphorylated 30 min after adhesion to CI in the control cells (Figure 9A); however, ERK phosphorylation only occurred at 60 min in the *Pkhd1*-silenced IMCD cells. The phosphorylation in the *Pkhd1*-silenced IMCD cells never reached the levels of the wild-type/control cells.

To test FAK phosphorylation activities, lysates of the cells obtained after adhesion to CI was screened with antibodies against the major phosphorylation sites of FAK, including FAKpY397, 407, 576, 577, and 861. Surprisingly, the only

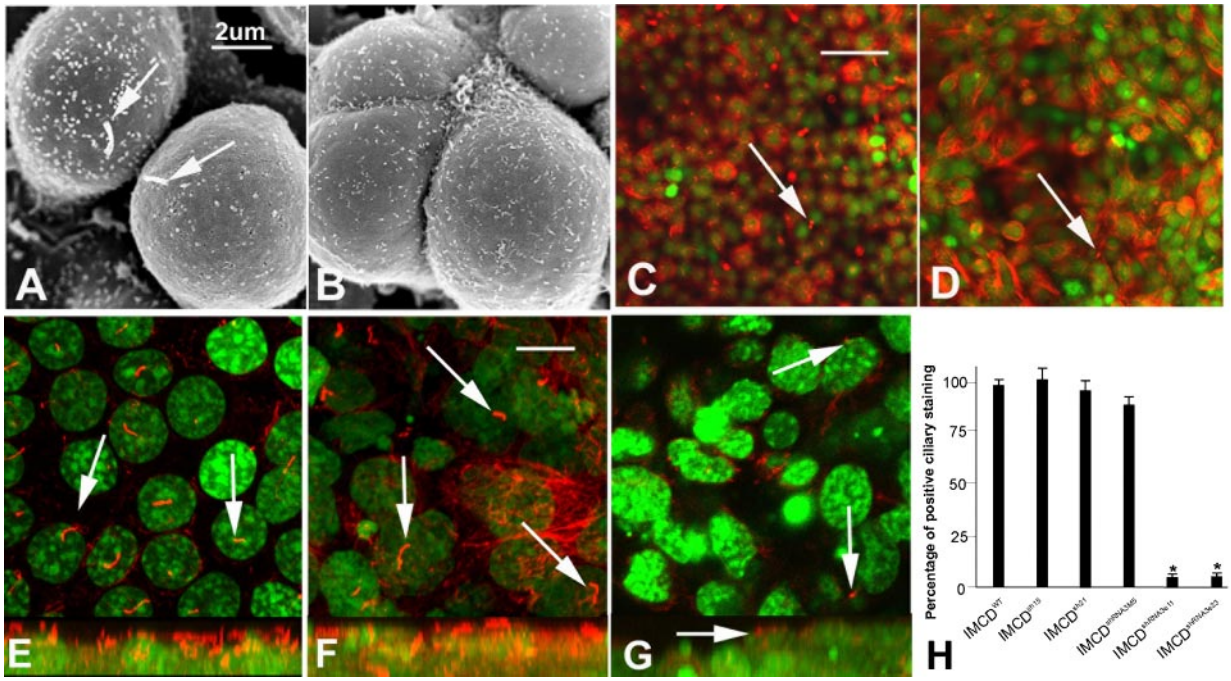

Figure 8. Inhibition of FPC arrested ciliogenesis in cultured *Pkhd1*-silenced IMCD cells. (A) SEM showed that the primary cilia (arrows in A) of cultured wild-type IMCD cells. (B) The ciliary structure disappeared in majority of *Pkhd1*-silenced IMCD cells under same cultured condition. (C–G) A common ciliary maker anti-acetylated α-tubulin antibody was used to stain the tested cells in transwell culture. (C) Clear-cut ciliary structures were abundantly observed in wild-type IMCD cells. (D) Few ciliary staining was seen in *Pkhd1*-silenced IMCD cells ($IMCD^{shRNA3e23}$). Green YO-PRO was used for nucleic staining. The confocal images also showed a significant decreased and shorten ciliary structure (arrows in E–G) in $IMCD^{shRNA3e23}$ cells (G) compared with control cell lines $IMCD^{sh21}$ (E) and $IMCD^{shRNA3M5}$ (F). The confocal lateral views (lower sections in E–G) were composed by multiple sections (~0.5-μm thick and up to 16 layers) which were projected onto one plane for presentation of ciliary staining patterns. (H) One hundred individual cells from five randomly picked high-power fields (1000×) were numbered; their ciliary staining and the positive cilium-staining rate are shown in H (* $p < 0.001$). Bars, (C–D) 15 μm, (E–G) 5 μm.

difference between the cell types was seen with FAKpY861, which showed markedly delayed and decreased phosphorylation in *Pkhd1*-silenced IMCD cells compared with wild-type/control cells (Figure 9, B and C). The results that both ERK1/2 and FAKpY861 phosphorylation are decreased in *Pkhd1*-silenced IMCD cells suggest that aberrant tubulomorphogenesis in vitro may be mediated by dysregulation of FAK and ERK activation.

DISCUSSION

FPC, the gene product of *PKHD1*, was deduced to be a receptor-like protein that may be involved in ligand-binding, cell-cell, and cell-matrix interactions (Onuchic *et al.*, 2002; Ward *et al.*, 2002). To date, no studies pertaining to the functional roles of this large and complex protein have been reported. In this in vitro study, utilizing stable *Pkhd1*-si-

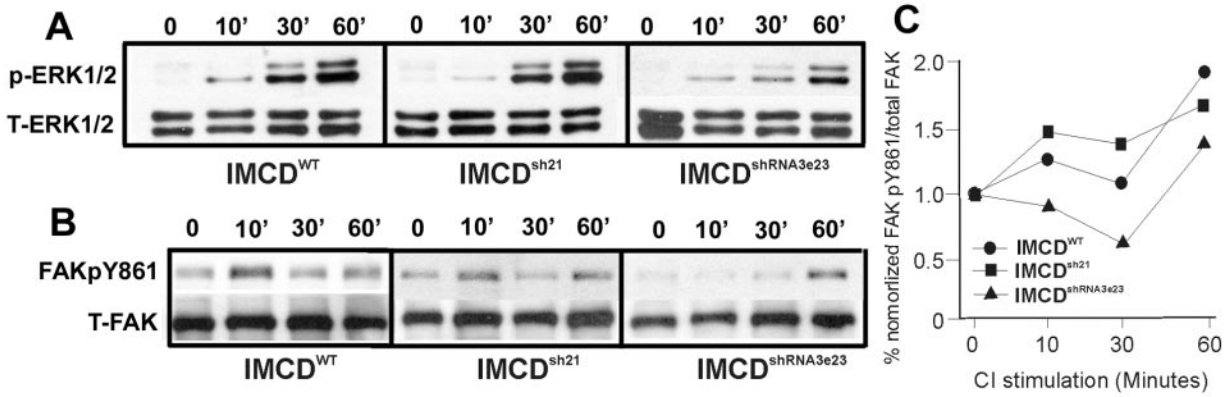

Figure 9. Pkhd1-silenced cells have decreased phosphorylation of ERK and FAK. Wild-type ($IMCD^{WT}$), vector control ($IMCD^{sh21}$), and *Pkhd1*-silenced ($IMCD^{shRNA3e23}$) cells were serum-starved for 12 h, trypsinized, and left in suspension or replated on 10 μg/ml collagen I for 10, 30, or 60 min. Equal amounts of cell lysate were separated by 10% SDS-PAGE and transferred to nitrocellulose. The membranes were immunoblotted with antibodies to phospho-ERK1/2 (p-ERK1/2) and total ERK (T-ERK1/2) (A) or phospho-FAKpY861 (FAKpY861) and total FAK (T-FAK) (B). A normalized quantitative analysis at the indicated times was performed using the densitometry values in the Western blots for FAK pY861 (C).

lenced IMCD cells, we demonstrated that down-regulating *Pkhd1* results in 1) the inhibition of tubulomorphogenesis; 2) impairment of cell-cell interactions and inducement of spontaneous cell scattering; 3) disorganization of the actin cytoskeleton and induction of EMT; 4) reduction of integrin-dependent adhesion; v) increased apoptosis and decreased cell proliferation; and 5) decreased FAKpY861 and ERK1/2 activation. Because FPC localizes at vicinity of the basobodies (centriole system) and the primary cilia (microtubule system) of epithelial cells (Masyuk *et al.,* 2003; Ward *et al.,* 2003; Menezes *et al.,* 2004; Wang *et al.,* 2004; Zhang *et al.,* 2004), dysfunction of FPC may potentially disrupt the core pathway for cytoskeleton distribution/assembly and disable scaffold protein transport for cell polarity generation, which might account for the diversity of cell biological alterations observed in our in vitro study.

A prominent biological defect found in the *Pkhd1*-silenced IMCD cells was the disruption of normal cell-cell interactions. The loss of E-cadherin-mediated cell-cell adhesion blocks the assembly of adherens junctions which is required for all other intercellular junction formation in cultured MDCK cells (Matter and Balda, 2003). Nevertheless, normal assembly of these intercellular junctions is essential for tubulogenesis (Grisendi *et al.,* 1998; Balda and Matter, 2003). In addition, defects in cell-cell adhesion were able to promote spontaneous cell scattering phenotypes and induce a failure in collective migration or migratory polarity of the renal epithelial cells, which is critical for normal tubule formation (Zegers *et al.,* 2003).

The failure of renal epithelia to assemble primary cilia induces cystogenesis in the kidneys (Yoder *et al.,* 2002; Lin *et al.,* 2003). Our in vitro findings suggested that ciliary generation was disrupted in *Pkhd1*-silenced IMCD cells, implicating possible FPC involvement in ciliogenesis. This result is consistent with a report that transiently siRNA-mediated inhibition of *Pkhd1* in chlolangiocytes resulted in shortening and decreased formation of cilia (Masyuk *et al.,* 2003). However, a mouse model with an exon 40 deletion of *Pkhd1*, which caused distinct liver cysts, did not show any ciliary abnormality in chlolangiocytes, suggesting that a lack of functional PFC may not affect normal ciliogenesis in vivo (Moser *et al.,* 2005). In spite of the spatial and environmental differences between the in vivo tissues and in vitro culture systems, the ciliary defect seen in cultured *Pkhd1*-silenced IMCD cells may be caused by arrestment of epithelial polarity, which may occur because of disruption of cytoskeleton organization, cell-cell/matrix contacts, and centriole arrangement.

The aberrant cell behaviors including abnormal proliferation, cell scattering, and disrupted cell-cell/matrix contacts can be mediated through several signal-transduction processes (Matter and Balda, 2003; Wozniak *et al.,* 2004). The down-regulation of JNK/SAPK phosphorylation induces cell scattering and the activation of ERK and PKB/Akt regulates epithelial tubulogenesis in cultured cells (Paumelle *et al.,* 2000; O'Brien *et al.,* 2004; Lavenburg, 2003). In addition, focal adhesive kinase (FAK) has been indicated to play a role in reorganization of the cytoskeleton, assembly of cell adhesion structures, and regulation of cell membrane protrusions to cell migration (Schaller, 2004). In our studies, we found a significant difference in the ERK signaling pathway, which has been implicated as a key regulator for cell proliferation (Roux and Blenis, 2004) and epithelial tubule formation in vitro (O'Brien *et al.,* 2004). Thus the aberrant proliferation and impairment of tubulomorphogenesis found in cultured *Pkhd1*-silenced IMCD cells may be mediated by disturbances of ERK signaling.

The observation that a difference in FAK phosphorylation was present at pY861 was intriguing. FAK is a protein tyrosine kinase that contains multiple critical tyrosine phosphorylation sites that could contribute to its central role in cell-cell/matrix contacts, cytoskeleton remodeling, cell scattering, and polarization (Mitra *et al.,* 2005). FAK is required for normal mouse developmental morphogenesis (Ilic *et al.,* 1995). Furthermore lack of FAK results in abnormalities in endothelial tubulogenesis in a 3-D cultured system (Ilic *et al.,* 2003). The fact that FAKpY861 was less phosphorylated may unveil a novel pathway that links FAK/ERK signaling to tubulomorphogenesis (Juliano, 2002; O'Brien *et al.,* 2004; Mitra and Hanson, 2005).

In addition, our results have also showed that normal cell-cell/matrix contacts in cultured *Pkhd1*-silenced IMCD cells have been impaired. It is feasible that loss of normal cell-cell/matrix contacts could disrupt junction-related gene expression (Balda and Matter, 2003). This disruption may dysregulate many cytoplasmic proteins, including transcriptional factors and/or other proteins that control cell-cycle progression, cytoskeleton remodeling, and epithelial polarization either directly or through other intermediary molecules, and eventually impair normal cell behaviors, including the multiple abnormalities observed in this study.

In our studies, we adopted a shRNA inhibition approach to knock down *Pkhd1* expression. We utilized an empty-vector control, $IMCD^{sh}$ and a mutagenized control, $IMCD^{shRNA3M}$, in which two base pairs in the middle of the hairpin duplexes were mutagenized to emphasize the specificity of our knockdown construct (Figure 2A). The use of the empty-vector $IMCD^{sh}$ cells was to prevent *Pkhd1*-specific micro-RNA effects, which may be produced by the $IMCD^{shRNA3M}$ construct (Ambros, 2004). This indeed appeared to be the case in our studies as the mutagenized $IMCD^{shRNA3M}$ cells exhibited a slightly decreased *Pkhd1* expression (Figure 2, F and M), resulting in minor alterations of E-cadherin and ZO-1 staining patterns (Figure 4, Ac and Bc). However, these graded changes from *Pkhd1*shRNA3 to *Pkhd1*shRNA3M and finally to $IMCD^{sh}$ provided further evidence for the silencing specificity of our *Pkhd1*shRNA3 construct.

In summary, we have demonstrated that down-regulation of FPC disrupts normal cell-cell and cell-ECM interactions of epithelial cells and promotes spontaneous cell scattering. In addition, it results in alterations in the cell proliferation, apoptosis, polarity, and cytoskeleton organization, which may be mediated by FAK and ERK signaling. As a consequence of some or all of these changes in cell biological processes, *Pkhd1*-silenced IMCD cells results in inhibition of tubulomorphogenesis in vitro. Given that FPC is expressed in the organs with primary duct systems, including the kidney, lung/trachea, mammary gland, cardiovascular system, and gastrointestinal/urinary-genital tracts, and is predominantly distributed at the apical domain of epithelial cells (Nagasawa *et al.,* 2002; Zhang *et al.,* 2004), this protein may serve as a key molecule for creating and/or maintaining the lumen of tubules/ducts. Disruption of this functional molecule gives rise to a pathogenic path for cystogenesis of ARPKD, in which massive fusiform ectasia of renal tubules is seen.

ACKNOWLEDGMENTS

We thank Drs. Alfred George, Steven Hanks, Zhizhuang Joe Zhao, Cunxi Li, and Ming-Zhi Zhang for their critical reading of the manuscript and suggestions and Daniel Kim for his excellent assistance in electron microscopy. This work was supported by a Veterans Administration Advanced Career Devel-

opment and Merit Award, an American Heart Association Grant in Aid Award, RO1 DK069921 and a Clinician Scientist award from National Kidney Foundation to R.Z. and grants from the Polycystic Kidney Research Foundation, the American Heart Association, and National Institutes of Health (DK062373 and DK062511) to G.W.

REFERENCES

Ambros, V. (2004). The functions of animal microRNAs. Nature *431*, 350–355.

An, J., Chen, Y., Huang, Z. (2004). Critical upstream signals of cytochrome C release induced by a novel bcl-2 inhibitor. J. Biol. Chem. *279*, 19133–19140.

Balda, M. S., and Matter, K. (2003). Epithelial cell adhesion and the regulation of gene expression. Trends Cell Biol. *13*, 310–318.

Berridge, M. V., Tan, A. S., McCoy, K. D., and Wang, R. (1996). The biochemical and cellular basis of cell proliferation assays that use tetrazolium salts. Biochemica *4*, 12–20.

Boletta, A., Qian, F., Onuchic, L. F., Bhunia, A. K., Phakdeekitcharoen, B., Hanaoka, K., Guggino, W., Monaco, L., Germino, G. G. (2002). Polycycstin-1, the gene product of PKD1, induces resistance to apoptosis and spontaneous tubulogenesis in MDCK cells. Mol. Cell *6*, 1267–1273.

Bosniak, M. A., and Ambos, M. A. (1975). Polycystic kidney disease. Semin. Roentgenol. *10*, 133–143.

Cai, S., Bulus, N., Fonseca-Siesser, P. M., Chen, D., Hanks, S. K., Pozzi, A., and Zent, R. (2005). CD98 modulates integrin beta1 function in polarized epithelial cells. J. Cell Sci. *118*, 889–899.

Chen, D., Roberts, R., Pohl, M., Nigam, S., Kreidberg, J., Wang, Z., Heino, J., Ivaska, J., Coffa, S., Harris, R. C., Pozzi, A., and Zent, R. (2004). Differential expression of collagen and laminin binding integrins mediate ureteric bud and inner medullary collecting duct cell tubulogenesis. Am. J. Physiol. Renal Physiol. *287*, F602–F611.

Grisendi, S., Arpin, M., and Crepaldi, T. (1998). Effect of hepatocyte growth factor on assembly of zonula occludens-1 protein at the plasma membrane. J. Cell. Physiol. *176*, 465–471.

Guay-Woodford, L. M. (1996). Autosomal recessive disease: clinical and genetic profiles. In: Polycystic Kidney Disease, ed. V. Torres, M. Watson, Oxford: Oxford University Press, 237–267.

Guay-Woodford, L. M. *et al.* (1995). The severe perinatal form of autosomal recessive polycystic kidney disease maps to chromosome 6p21.1-p12, implications for genetic counseling. Am. J. Hum. Genet. *56*, 1101–1107.

Hanks, S. K., Calalb, M. B., Harper, M. C., and Patel, S. K. (1992). Focal adhesion protein-tyrosine kinase phosphorylated in response to cell attachment to fibronectin. Proc. Natl. Acad. Sci. USA *89*, 8487–8491.

Higashiyama, S., Iwamoto, R., Goishi, K., Raab, G., Taniguchi, N., Klagsbrun, M., and Mekada, E. (1995). The membrane protein CD9/DRAP 27 potentiates the juxtacrine growth factor activity of the membrane-anchored heparin-binding epidermal growth factor-like growth factor. J. Cell Biol. *128*, 929–938.

Ilic, D., Furuta, Y., Kanazawa, S., Takeda, N., Sobue, K., Nakatsuji, N., Nomura, S., Fujimoto, J., Okada, M., and Yamamoto, T. (1995). Reduced cell motility and enhanced focal adhesion contact formation in cells from FAK-deficient mice. Nature *377*, 539–544.

Ilic, D., Kovacic, B., McDonagh, S., Jin, F., Baumbusch, C., Gardner, D. G., and Damsky, C. H. (2003). Focal adhesion kinase is required for blood vessel morphogenesis. Circ. Res. *92*, 300–307.

Juliano, R. L. (2002). Signal transduction by cell adhesion receptors and the cytoskeleton: functions of integrins, cadherins, selectins, and immunoglobulin (Ig)-superfamily members. Annu. Rev. Pharmacol. Toxicol. *42*, 283–323.

Lavenburg, K. R., Ivey, J., Hsu, T., Muise-Helmericks, R. C. (2003). Coordinated functions of Akt/PKB and ETS1 in tubule formation. FASEB J. *17*, 2278–2280.

Lin, F., Hiesberger, T., Cordes, K., Sinclair, A. M., Goldstein, L. S., Somlo, S., and Igarashi, P. (2003). Kidney-specific inactivation of the KIF3A subunit of kinesin-II inhibits renal ciliogenesis and produces polycystic kidney disease. Proc. Natl. Acad. Sci. USA *100*, 5286–5291.

Masyuk, T. V. *et al.* (2003). Defects in cholangiocyte fibrocystin expression and ciliary structure in the PCK rat. Gastroenterology *125*, 1303–1310.

Matter, K., and Balda, M. S. (2003). Signalling to and from tight junctions. Nat. Rev. Mol. Cell. Biol. *4*, 225–236.

Menezes, L. F., Cai, Y., Nagasawa, Y., Silva, A. M., Watkins, M. L., Da Silva, A. M., Somlo, S., Guay-Woodford, L. M., Germino, G. G., Onuchic, L. F. (2004). Polyductin, the PKHD1 gene product, comprises isoforms expressed in plasma membrane, primary cilium, and cytoplasm. Kidney Int. *66*, 1345–1355.

Mitra, S. K., Hanson, D. A., and Schlaepfer, D. D. (2005). Focal adhesion kinase: in command and control of cell motility. Nat. Rev. Mol. Cell. Biol. *6*, 56–68.

Moser, M., Matthiesen, S., Kirfel, J., Schorle, H., Bergmann, C., Senderek, J., Rudnik-Schoneborn, S., Zerres, K., and Buettner, R. (2005). A mouse model for cystic biliary dysgenesis in autosomal recessive polycystic kidney disease (ARPKD). Hepatology *41*, 1113–1121.

Mucher, G., Wirth, B., and Zerres, K. (1994). Refining the map and defining flanking markers of the gene for autosomal recessive polycystic kidney disease on chromosome 6p21.1-p12. Am. J. Hum. Genet. *55*, 1281–1284.

Nagasawa, Y. *et al.* (2002). Identification and characterization of Pkhd1, the mouse orthologue of the human ARPKD gene. J. Am. Soc. Nephrol. *13*, 2246–2258.

Nelson, W. J. (2003). Tube morphogenesis: closure, but many openings remain. Trends Cell Biol. *13*, 615–621.

O'Brien, L. E., Tang, K., Kats, E. S., Schutz-Geschwender, A., Lipschutz, J. H., and Mostov, K. E. (2004). ERK and MMPs sequentially regulate distinct stages of epithelial tubule development. Dev. Cell *7*, 21–32.

Onuchic, L. F. *et al.* (2002). PKHD1, the polycystic kidney and hepatic disease 1 gene, encodes a novel large protein containing multiple Ig-like plexin-transcription-factor domains and parallel beta-helix 1 repeats. Am. J. Hum. Genet. *70*, 1305–1317.

Paumelle, R., Tulasne, D., Leroy, C., Coll, J., Vandenbunder, B., and Fafeur, V. (2000). Sequential activation of ERK and repression of JNK by scatter factor/hepatocyte growth factor in madin-darby canine kidney epithelial cells. Mol. Biol. Cell *11*, 3751–3763.

Potter, E. L. (1972). Normal and abnormal development of the kidney. Year Book: Chicago.

Roux, P. P., and Blenis, J. (2004). ERK and p38 MAPK-activated protein kinases: a family of protein kinases with diverse biological functions. Microbiol. Mol. Biol. Rev. *68*, 320–344.

Schaller, M. D. (2004). FAK and paxillin: regulators of N-cadherin adhesion and inhibitors of cell migration? J. Cell Biol. *166*, 157–159.

Wang, S., Luo, Y., Wilson, P. D., Witman, G. B., and Zhou, J. (2004). The autosomal recessive polycystic kidney disease protein is localized to primary cilia, with concentration in the basal body area. J. Am. Soc. Nephrol. *15*, 592–602.

Ward, C. J. *et al.* (2002). The gene mutated in autosomal recessive polycystic kidney disease encodes a large, receptor-like protein. Nat. Genet. *30*, 259–269.

Ward, C. J. *et al.* (2003). Cellular and subcellular localization of the ARPKD protein; fibrocystin is expressed on primary cilia. Hum. Mol. Genet. *12*, 2703–2710.

Woo, D. (1995). Apoptosis and loss of renal tissue in polycystic kidney diseases. N. Engl. J. Med. *333*, 18–25.

Wozniak, M. A., Modzelewska, K., Kwong, L., and Keely, P. J. (2004). Focal adhesion regulation of cell behavior. Biochim. Biophys. Acta *1692*, 103–119.

Xiong, H. *et al.* (2002). A novel gene encoding a TIG multiple domain protein is a positional candidate for autosomal recessive polycystic kidney disease. Genomics *80*, 96–104.

Yoder, B. K., Tousson, A., Millican, L., Wu, J. H., Bugg, C. E., Jr., Schafer, J. A., and Balkovetz, D. F. (2002). Polaris, a protein disrupted in orpk mutant mice, is required for assembly of renal cilium. Am. J. Physiol. Renal. Physiol. *282*, F541–F552.

Zegers, M. M., O'Brien, L. E., Yu, W., Datta, A., and Mostov, K. E. (2003). Epithelial polarity and tubulogenesis in vitro. Trends Cell Biol. *13*, 169–176.

Zent, R., Bush, K. T., Pohl, M. L., Quaranta, V., Koshikawa, N., Wang, Z., Kreidberg, J. A., Sakurai, H., Stuart, R. O., Nigam, S. K. (2001). Involvement of laminin binding integrins and laminin-5 in branching morphogenesis of the ureteric bud during kidney development. Dev. Biol. *238*, 289–302.

Zerres, K., Rudnik-Schoneborn, S., Steinkamm, C., Becker, J., and Mucher, G. (1998). Autosomal recessive polycystic kidney disease. J. Mol. Med. *76*, 303–309.

Zhang, M. Z. *et al.* (2004). PKHD1 protein encoded by the gene for autosomal recessive polycystic kidney disease associates with basal bodies and primary cilia in renal epithelial cells. Proc. Natl. Acad. Sci. USA *101*, 2311–2316.